Contents lists available at SciVerse ScienceDirect

Ultrasonics Sonochemistry

journal homepage: www.elsevier.com/locate/ultsonch

Sono-synthesis of core–shell nanocrystal (CdS/TiO₂) without surfactant

Narjes Ghows, Mohammad H. Entezari *

Department of Chemistry, Ferdowsi University of Mashhad, 91775 Mashhad, Iran

ARTICLE INFO

ABSTRACT

A core–shell nanocomposite (CdS/TiO₂) was synthesized at relatively low temperature (70 °C) with small particle sizes (∼11 nm). First, CdS nanoparticles were prepared by a combination of ultrasound and new micro-emulsion (O/W) without surfactant. Then the synthesized CdS was easily combined with TiO₂ under sonication. The formation of uniform surface layer of TiO₂ with depths of 0.75–1.1 nm on the CdS led to an increase of particle size. Ultrasonic irradiation can control the hydrolysis and condensation of titanium tetra-isopropoxide (TTIP) and the formation of TiO₂ shell around the CdS core. This technique avoids some of the problems that exist in conventional microemulsion synthesis such as the presence of different additives and calcinations. It was found that nanocomposite particles extend the optical absorption spectrum into the visible region in comparison with pure TiO₂ and pure CdS. In addition, a larger depth of TiO₂ led to a red-shift of the absorption band in nanocomposite. The characterization of nanocomposites has been studied by HRTEM, TEM, XRD, EDAX, BET and, UV–vis.

© 2012 Elsevier B.V. All rights reserved.

1. Introduction

The properties of core–shell composite materials are combination of the properties of both materials in the core and shell. These materials have attracted increasing interest to material scientists due to their great potential applications, unique size, shape-dependent optical and electronic properties in both fundamental research and industrial development. This is due to their potential applications in photovoltaic cells, optical sensor device photocatalysts, and catalysts [1–5]. They can also compensate for the disadvantages of the individual components. In one successful approach, a thin shell of a wide band-gap semiconductor has been deposited on a small band gap semiconductor. This can induce a synergistic effect such as an efficient charge separation and improvement of photostability [1,6] with respect to the single phase. But, uniform deposition of inorganic material on small core particles is often problem due to the lack of coating methods and poor surface interactions under the usual experimental conditions. On the other hand, in conventional synthesis of the coupled semiconductors, long aging times (at least 20–24 h) and high temperatures (200–400 °C) are required for improving the contact of the two components and their crystallinity [4,6–9]. Hence, developing novel facile preparation methods under mild and easy conditions is still a challenge for both industry and academic works [10,11].

A new sonochemical method for the deposition of TiO₂ on CdS nanoparticles was designed to overcome these problems. The synthesis of uniform and narrow size nanoparticles with ultrasound is an easy and more effective method under mild conditions [12–14]. During the irradiation of liquids with ultrasound, the extreme local conditions caused by acoustic cavitation (5000 K, 500 bar) [15] not only decompose organometallic precursors to form nano-sized inorganic particles [16–18], but also facilitate the crystallization of the semiconductors [19]. This is due to the high temperature and pressure produced during the cavitation. It is also possible to facilitate the formation of core–shell nanomaterial with the uniform deposition of the nanosized inorganic particles onto another surface by ultrasound [14,20–23]. The removal of surface contaminants helps the inorganic clusters to adhere more uniformly [14,18] in comparison with those reported without ultrasound [24]. There are relatively rare reports on the formation of core–shell-particles (CdS–TiO₂) by using ultrasound. The sonochemical formation of CdS–TiO₂ core–shell has been reported with hexagonal phase in the range of 25–30 nm under multibubble sonoluminescence (MBSL) condition [25].

Our recent works confirmed that the synthesis of nanoparticles is easier with ultrasound than other methods [21,26–28]. It seems that the combination of ultrasound and micro-emulsion is a suitable method for the synthesis of semiconductors with core–shell structure. This combination could be useful for the uniform deposition and the control of crystal phase, morphology, and size of the nano-particles. In this investigation, a new method has been developed for the preparation of CdS/TiO₂ nanocomposite (core/shell) with sizes smaller than 11 nm by using ultrasonic waves under mild conditions. Also, this method avoids some problems that exist in microemulsion system like the presence of different surfactants and calcinations.

---

* Corresponding author.
  E-mail address: moh_entezari@yahoo.com (M.H. Entezari).

To the best of our knowledge, there is no report on the preparation of CdS/TiO$_2$ nanocomposite by a combination of ultrasound and microemulsion without the use of a surfactant. In this study, CdS nanoparticles were combined with TiO$_2$ for the synthesis of core/shell type nanocrystals, through a simple sonochemical reaction in microemulsion medium without additives. The product was prepared under mild conditions with uniform deposition and most importantly without any post thermal treatment. It seems that this procedure can be easily generalized for the preparation of other core–shell nanosemiconductor materials.

2. Materials and methods

2.1. Materials

Ethylenediamine, titanium tetra-isopropoxide (TTIP) from Merck, CS$_2$, CdCl$_2$, 2H$_2$O from Fluka have been used without further purification. De-ionized water was used for the sample preparation.

2.2. Procedure

2.2.1. Synthesis of core–shell nanoparticles

First, ethylendiamine (0.6 mL) was dissolved in water (40 mL) in a Rosset Cell at about 288 K. Then, CS$_2$ (0.2 mL) was introduced into the solution as an oil phase. The mixture was irradiated with ultrasound (20 kHz Sonifier W-450, amplitude% 75, normal horn, acoustic power, 41 W) at about 35 °C. The turbid solution became clear after ∼2 min sonication. Then an aqueous solution of cadmium chloride (CdCl$_2$ 2H$_2$O, 0.15 g dissolved in 10 mL solution) was introduced into the cell and it was sonicated for another 10 min at the same temperature. In another step by stopping the circulating bath during sonication, the temperature was increased from 35 to 70 °C and the nucleation processes were began after 5 min. After 30 min sonication, then 0.4 mL and 1.0 mL titanium isopropoxide were added in separate experiments drop by drop (the mole ratio of TiO$_2$ to CdS was 2.5 and 6.0). Then, sonication continues for 1.5 h by controlling temperature (70–73 °C). The precipitate was separated by centrifugation (10000 rpm in 10 min.), washed with distilled water and then two times with absolute ethanol, and then dried at room temperature. The final product with mole ratio 2.5 was green.

2.2.2. Synthesis of TiO$_2$ nanoparticles

Nanocrystalline TiO$_2$ was synthesized by hydrolysis of titanium tetra-isopropoxide (TTIP) in de-ionized water under ultrasonic irradiation (20 kHz, 41 W). In this experiment, 1 mL TTIP was injected drop-wise into 50 mL of de-ionized water. The mixture was sonicated continuously for 1.5 h under ambient atmosphere. The sonication was conducted without cooling and the temperature was raised from 25 °C to about 70 °C at the end of the reaction. The obtained precipitates were separated by centrifugation (15000 rpm in 20 min) and washed with de-ionized water and ethanol several times. The product was dried at room temperature.

2.3. Characterization of the core–shell nanoparticles

The structure and morphology of the products have been studied by transmission electron microscopy (HRTEM, Hi-TEM is Hitachi 300 kV H-9500 TEM with accelerate voltage 300–100 kV and resolution 0.1 nm for crystal lattice and 0.18 nm for point to point). The X-ray diffraction (XRD) patterns were recorded in a wide angle range (2θ = 10 –70) by Bruker-AXS, D8 Advance in scanning step of 0.02°/sec, with monochromatized CuKα radiation (λ = 1.5406 Å). The optical properties of the core–shell nanoparticles were studied by UV–Vis spectroscopy (Unico 2800). The surface area measurement (BET) was determined by MONOSORB and the out-gassing of the samples was done at 65 °C for 3 h. The energy dispersed analysis of X-ray (EDAX) was carried out using a Philips, XL30 model.

3. Results and discussion

3.1. Mole ratio of CdS/TiO$_2$

Fig. 1A shows the XRD patterns of CdS/TiO$_2$ nanocrystal at two different mole ratios and each component individually. The XRD patterns reveal that CdS nanoparticles are in hexagonal phase with the most intense peaks at 2θ = 24.7°, 26.5°, 28.3°, 43.8°, 48.1° and 51.8° which correspond to (100), (002), (101), (110), (103) and (112) planes, respectively. The most intense peaks at angles (2θ) = 25.1°, 48.1°, 62.5° correspond to the (101), (200), (204) planes of the anatase phase of TiO$_2$. The relatively low intensities and broadness of X-ray diffraction peaks are assumed to arise from the fact that particles are nano-sized and a low thickness of TiO$_2$ was formed on the CdS nanoparticles. The mean crystallite size diameter (D) of the CdS, TiO$_2$, and composite nanoparticles was estimated by Scherrer's equation (Table 1).

The samples prepared at ratio 2.5:1 and 6:1 show the main peak of the anatase phase of TiO$_2$ as a weak peak which is due to low thickness of TiO$_2$ shell or a high dispersion of TiO$_2$ with the less crystallinity on the CdS [21,25,29]. Reduction of the intensity of CdS peaks in the composite might be related to the presence of low amount of TiO$_2$ on the CdS. Fig. 1B shows the main peak of the anatase TiO$_2$ phase with low crystallinity.

Fig. 2 presents the HRTEM and TEM images of CdS and core–shell nanoparticles. It was clearly demonstrated that a nanoshell was formed on the CdS nanoparticles. The average size of the bare CdS nanoparticles was about 8–10 nm in diameter and those of core–shell nanoparticles were found to be in the range of 9.84–11 nm, indicating that the coating depth is about 0.75–1.1 nm. In contrast to the ultrasonic method, under the normal experimental conditions the uniform deposition of inorganic material on small core particles is often problematic due to the lack of coating methods and poor surface interactions [14]. In fact, rapid synthesis with uniform deposition of TiO$_2$ on CdS nanoparticles under the described sonochemical conditions might be attributed to the physical and chemical effects of cavitation. In addition, the rate of hydrolysis of TTIP became highly accelerated by several orders in the presence of ultrasound [23,25].

In contrast, the TTIP hydrolysis in the presence of CdS NPs under stirring (similar condition with ultrasound) causes formation of large irregular aggregates with the extremely heterogeneous distribution. Hence, the treatment of solutions with power ultrasound not only facilitates the dispersion of solids in the liquids but also provides a unique set of conditions for uniform coating. The chemical composition analysis of the coupled semiconductor by EDAX revealed that the core–shell nanocrystal has a high purity and the ratio of Cd/S is nearly 1:1, and that of TiO$_2$/CdS is about 2.5:1 (Fig. 2f).

3.2. Preparation methods

The preparation method plays an important role on the structure and properties of the composites. Three methods were applied for the synthesis. The first method (a) was explained in the materials and methods section. In the second method (b), nanocrystalline TiO$_2$ was synthesized by the hydrolysis of titanium tetra-isopropoxide (TTIP) in de-ionized water under ultrasonic irradiation (20 kHz, 41 W). In a typical synthesis, 1 mL TTIP was injected drop-wise into the 50 mL of de-ionized water. The mixture
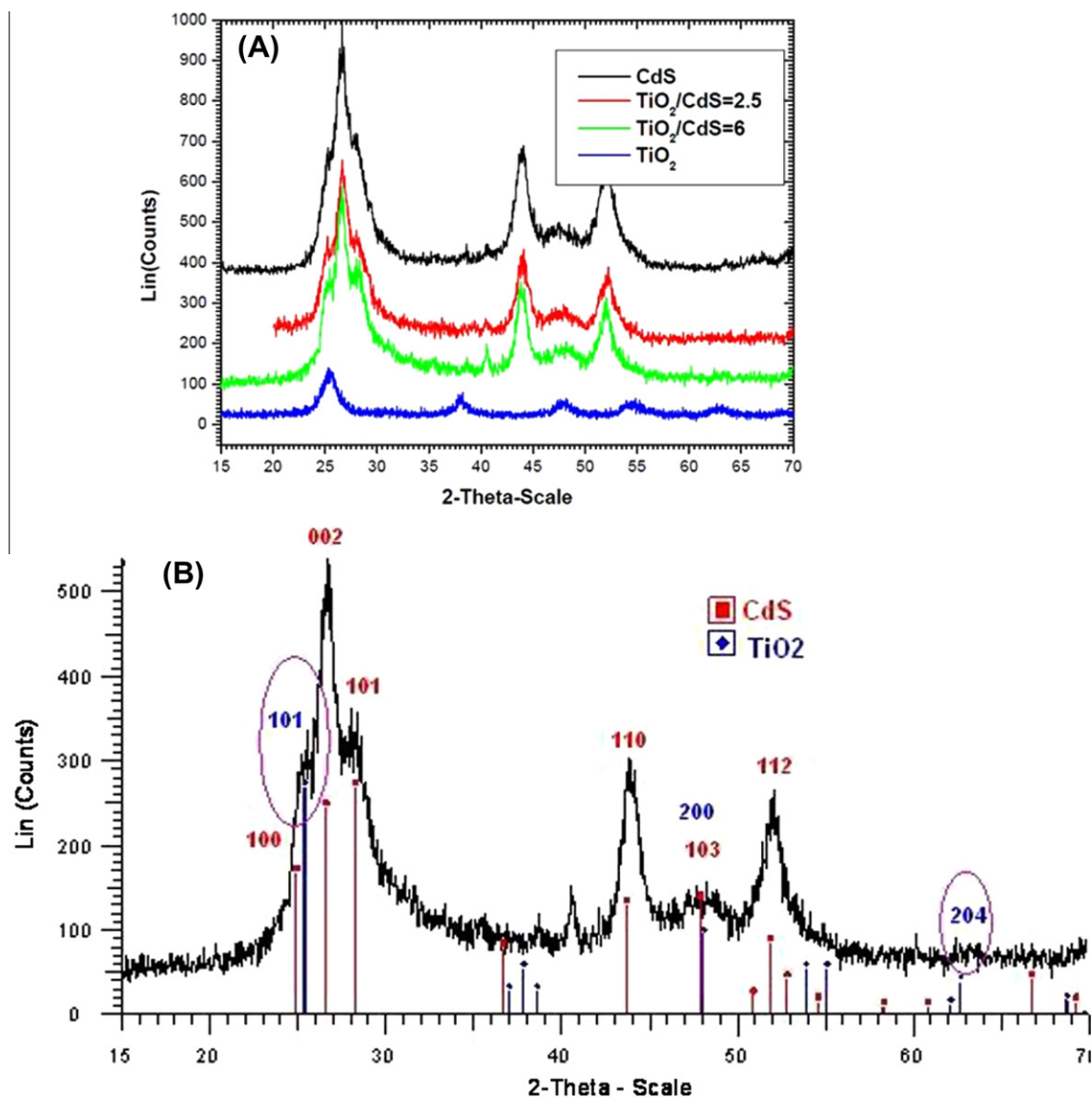
Fig. 1. (A) X-ray diffraction patterns of the samples with different molar ratios, (B) X-ray diffraction pattern of the sample with molar ratio of 6.0:1 (irradiation time 2 h).

Table 1
Surface and size of nano-particles.

Sample	Size (XRD)[a] (nm)	Size (TEM) (nm)	Surface area (m²/g)
CdS	6.9	<10	119 ± 3
TiO₂/CdS = 2.5	8.3	9.84–11	226 ± 4
TiO₂/CdS = 6	8.5	–	15.8 ± 0.3
TiO₂	10.9	–	379 ± 2

[a] The size was deduced from the full width at half maximum of the second sharp peak. It was the size of CdS rather than that of the composite.

was sonicated for 1.5 h under ambient conditions. The sonication was conducted without cooling system and the temperature was raised from 25 °C to ~70 °C at the end. Then 0.09 g CdS (obtained by method "a") was added to the mixture and sonication was continued for another 30 min. The obtained precipitates were separated by centrifugation (10000 rpm in 10 min.) and washed with de-ionized water and ethanol several times. The product was dried at room temperature. In the third method (c), 0.09 g CdS (obtained by method "a") was added to the 50 mL of de-ionized water and sonicated for 10 min. Then 1 mL TTIP was injected drop-wise to

the mixture and sonicated for 1.5 h under ambient atmosphere (the temperature was raised from 25 °C to ~70 °C at the end of the reaction). The obtained precipitates were separated by centrifugation (10000 rpm in 10 min) and washed with de-ionized water and ethanol several times. The product was dried at room temperature.

The crystalline phases of the products were determined by X-ray diffraction. The products were different in method (b and c) than method (a) (Fig. 3(A), Table 2). Fig. 3(B and C) shows the chemical composition analysis of the coupled semiconductor that was examined by EDAX. Signals corresponding to Ti, Cd and S were detected in all of the samples. The EDAX results revealed the presence of CdS with a higher content in sample (c) and lower content of CdS in sample (a). These data clearly confirmed that the products are CdS–TiO₂ composite nanoparticles. The elemental analysis was in agreement with the ratio of Cd/S which is nearly 1:1, and that of TiO₂/CdS which is about 6:1.

In the UV–vis absorption spectra, the three samples prepared with different methods were compared with a sample as a mixture of two components with the same ratio. The spectrum of the mixed sample showed a combination of the two separate spectra of CdS
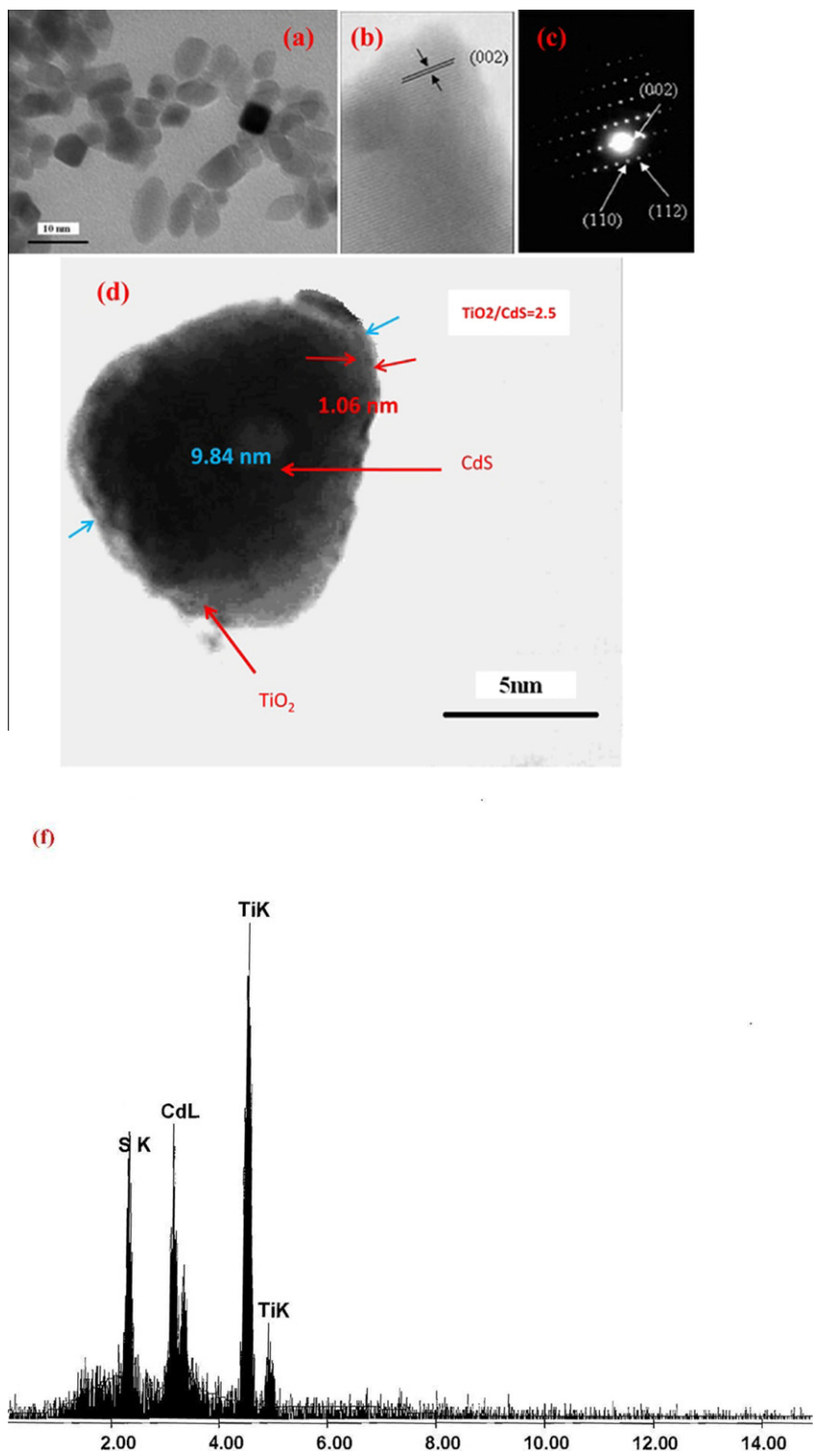
Fig. 2. Pure CdS synthesized by ultrasound in 30 min a) TEM, (b) HRTEM image and (c) SAED; nanocomposite under ultrasound in 2 h (d) HRTEM image of the sample and (f) EDAX with molar ratio = 2.5:1.

and TiO$_2$ nanoparticles which is different than the samples prepared by other methods. These differences should be attributed to the different structures of the nanoparticles (Fig. 4).

The control experiments for the synthesis have been done with stirring method for only CdS and TiO$_2$ and the results are available in our recent works [21,27,28]. The results showed that the TiO$_2$ particles are amorphous in nature (Fig. 1b [27]). The liquid–liquid heterogeneous mixture of CS$_2$ and water in control experiment led to a low yield of CdS (Table 2 [28]). In addition, for the synthesis of

core–shell with surfactant, the SEM and TEM images (Fig. 2c–e [21]) confirmed a heterogene coating on the core. Hence, control method cannot be a proper method for the preparation of selected nanoparticles.

3.3. UV–vis absorption

The UV–vis absorbance spectra of the pure and composite semiconductors are shown in Fig. 5a. The single-phase, CdS and
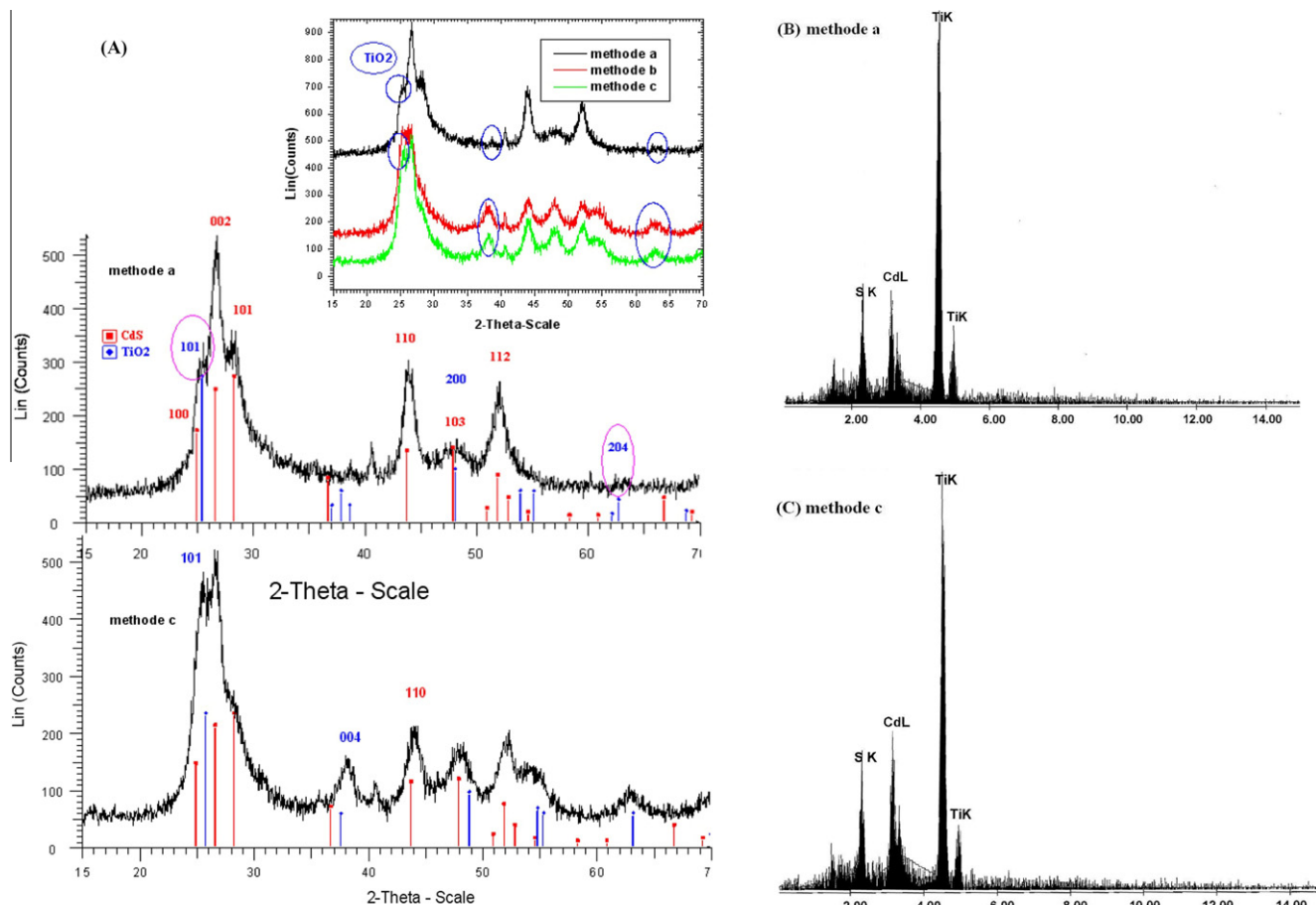
Fig. 3. (A) Effect of three different preparation methods on the structure of nanocomposite (a) sono- synthesis of CdS and then hydrolysis of TTIP under ultrasound, (b) sono-synthesis of TiO₂ and then its coating with CdS powder under ultrasound, (c) Adding of CdS powder and then hydrolysis of TTIP under ultrasound (B) EDAX sample (a) and (C) EDAX sample (c).

Table 2
XRD characteristics and surface area of nanocomposites prepared under ultrasound with different methods.

TiO₂/CdS = 6	Surface area (m²/g)	Intensity cps	FWHM degree	hkl	d^d (A°)	2θ Degree	Size^c (nm)
Method (a)	15.8 ± 0.3	292	1.0	110(H)^a	2.06	43.8	8.5
Method (b)	45.8 ± 0.9	188	1.1	110(H)^a	1.89	43.9	8.1
		174	0.9	004(A)^b	2.38	37.7	
Method (c)	213 ± 5	211	1.1	110(H)^a	2.06	43.9	8.0
		160	0.9	004(A)^b	2.38	37.7	

^{a} Hexagonal for CdS,
^{b} Anatase for TiO₂.
^{c} The size was deduced from the full width at half maximum of the second sharp peak related to CdS.
^{d} Distance of layers.

TiO₂ nanoparticles showed a band edge with E_g = 2.7 and E_g = 3.6 eV, respectively (Fig. 5c and d). In Fig. 5b, there are two clear transitions occurring at 2.3 eV and 3.1 eV which may be due to the participations of CdS and TiO₂ in the core–shell system respectively. Increasing the TiO₂ led to a red-shift of the absorption band in the composite and extends the optical absorption spectrum into the visible region in comparison with that of pure TiO₂ and pure CdS. The red shift of spectra is typical characteristics of core–shell nanocrystals with higher band gap shells, due to diminishing of the surface defects of core [5].

The E_g was determined by plotting $(\alpha h\nu)^2$ versus hν (Eq. (1)) and extrapolating the linear portion which intercepts the energy axis hν (Fig. 5b–d). The exponent n can take the value 1/2 or 2, for indirect and direct optical transition, respectively [9,30].

$$(\alpha h\nu)^2 = A(h\nu - E_g) \tag{1}$$

where α is the absorption coefficient, A and E_g are constant and band gap of the nanoparticle, respectively.

3.4. Comparison with and without surfactant

The addition of surface active materials (surfactants) to the colloidal solution influences the stability of nanoparticles. In some cases, there is a strong interaction between the surfaces of nanocrystals and surface active materials. The adsorption of surfactants on various crystallographic planes of the nanocrystals played a vital role in controlling the morphology and particle size of nanocrystals [31].
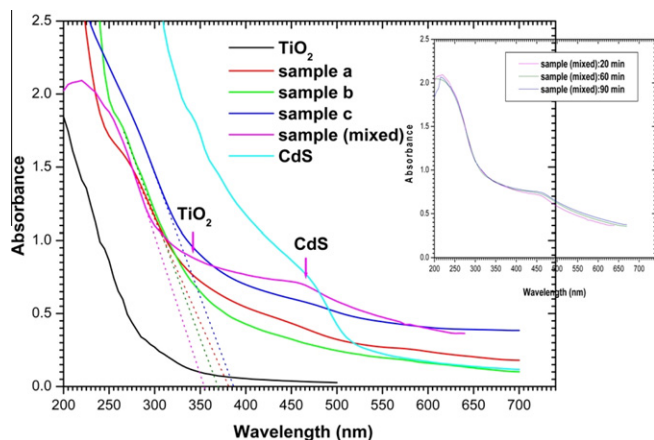
Fig. 4. The UV–vis absorbance spectra of three different preparation methods (insert: mixing of samples at different times).

On the other hand, the dispersion of semiconductor nanoparticles during ultrasonic treatment can be controlled by addition of surfactants [32]. Fig. 6 shows the XRD pattern, HRTEM image, and UV–vis absorbance spectra of the core–shell nano-composite prepared by combined method of microemulsion-ultrasound with surfactant (our recent work) [21] and compares with the sample prepared without surfactat. As it is shown in Fig. 6(b and c), the presence and absence of surfactant could affect the crystallinity

and the absorption band which is due to its growth and particle size. In the presence of surfactant, the particles have smaller size and more uniform [18] in comparison with core–shell nano-composite prepared without surfactant (Figs. 1b, 2d, and Table 3). This is due to strong interaction between the surfaces of nano-crystals and surfactant. In addition, the surface-active solutes in acoustic cavitation can influence the bubble/solution interface [33].

The XRD patterns also present stronger peaks without surfactant than those prepared with surfactant. This is probably due to the fact that alcohol into microemulsion with surfactant suppresses the hydrolysis of titanium alkoxide and rapid crystallization of the TiO_2 particles [34]. In addition, its vapor in the bubble affects the cavitational collapse and reduces the final temperature in an adiabatic compression [35]. As a result, the low temperature produced by the collapse of the cavities containing more alcohol leads to the less crystality nature of the product.

3.5. Effect of temperature

The temperature plays an important role in the formation, structure and size of the nanoparticles. The experiments were done at two different temperatures. According to Fig. 7, by increasing the temperature from 47 to 70 °C, the crystallinity of the sample improves. The increase of temperature leads to a higher mass transfer between the two phases which enhances the reaction rate, and formation of nanoparticles. On the other hand, the high temperature produced during cavitation can facilitate the crystalli-
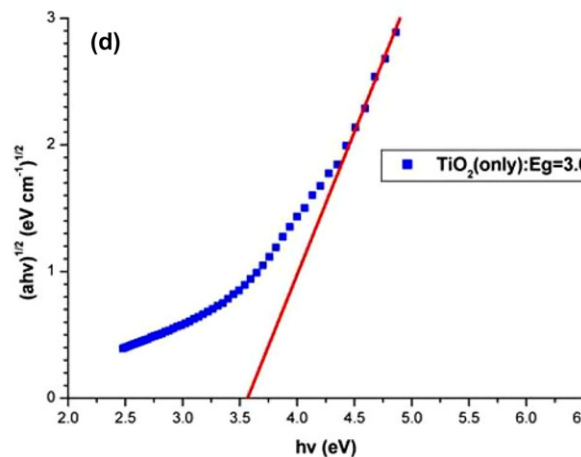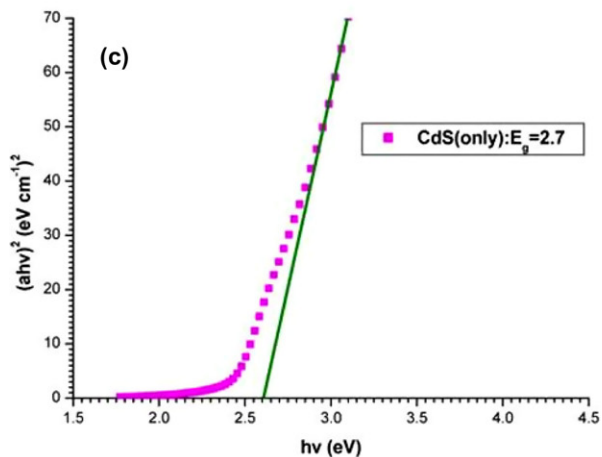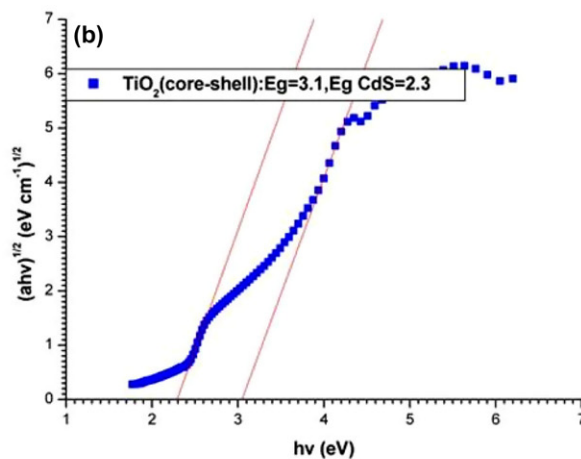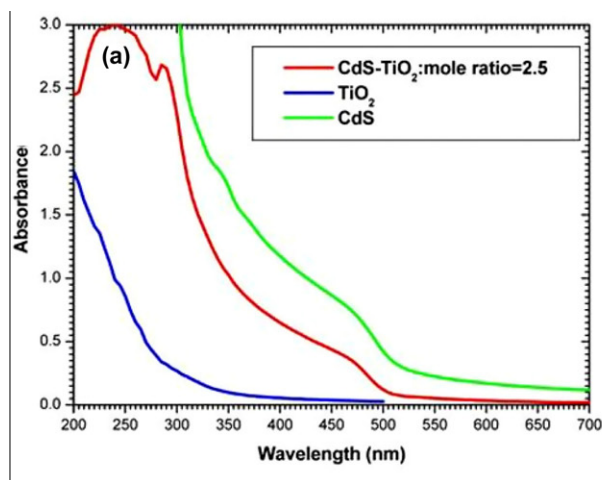

Fig. 5. The UV–vis absorbance spectra of pure and composite semiconductors (a), band gap of composite and pure semiconductors, respectively (b–d).
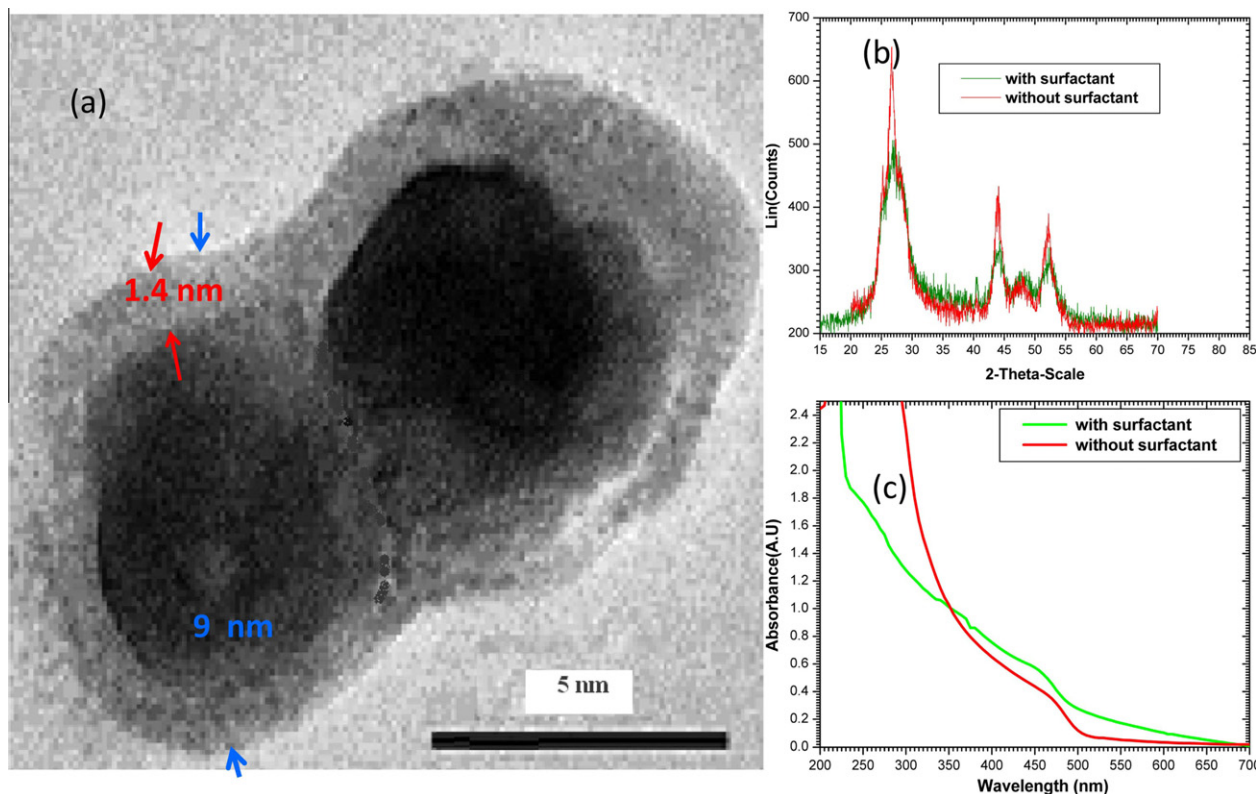
Fig. 6. HRTEM image of the sample prepared in the presence of surfactant with molar ratio, 2.5:1 (our recent work [21]) and XRD in the presence and absence of surfactant with molar ratio, 2.5:1.

Table 3
Effect of surfactant on the surface and size of nano-composite.

Sample	Size (XRD)[a] (nm)	Size (TEM) (nm)	Surface area (m²/g)
TiO₂/CdS = 2.5(without surfactant)	8.3	9.84–11	226 ± 4
TiO₂/CdS = 2.5(with surfactant) [21]	5.2	9–10	133 ± 3

[a] The size was deduced from the full width at half maximum of the second sharp peak related to CdS.

zation of the product. In this case, the interfacial zone of the cavity is a preferred region for the crystallization. This is due to the low vapor pressure of the reactants and also the achievement of a high temperature at this region. The cooling rate of the cavitation after

Fig. 7. Effect of temperature on the preparation.

collapsing is higher when the medium temperature is low. For the crystallization, a lower cooling rate is better than higher one. Therefore, sonication at higher temperature led to a higher crystallization. These arguments have been discussed previously by Suslick who has demonstrated that the higher cooling rates obtained during the collapse of the sonication bubble lead to the formation of amorphous products [36]. Also, Gedankan et al. proved that the reaction products are crystalline at high temperature while they are amorphous under low temperature [37].

3.6. Growth mechanism

The formation of CdS nano-particles is based on the reaction between CS₂ and ethylenediamine which present in two different phases. The chemical and physical effects of ultrasound arise from acoustic cavitation which is responsible for the mixed phase reactions, increases the surface area, and the mass transfer between two phases [28,38]. Therefore, in contrast to the stirring method, the liquid–liquid heterogeneous mixture of ethylenediamine, CS₂ and water can lead to a clear solution by ultrasound. The final clear solution behaves the same as a microemulsion but, without the use of surfactant. The CdS nanoparticles form with addition of cadmium ion to this solution at the oil–water interface. It may be attributed to the following reactions [39].
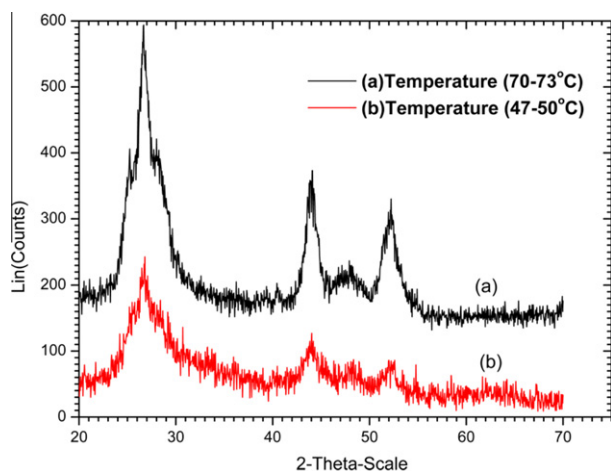
Fig. 8. Proposed model for the formation of CdS-TiO$_2$ nanocomposite with core–shell structure.

$$H_2N—CH_2—CH_2—NH_2 + CS_2 \rightarrow H_2N—CH_2—CH_2—NH—CS—SH$$

$$n(H_2N—CH_2—CH_2—NH—CS—SH) \rightarrow (—HN—CH_2—CH_2—NH—CS—)n + nH_2S$$
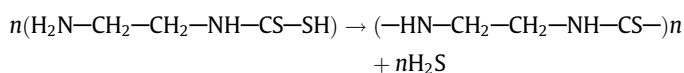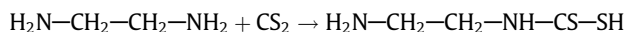
The turbulent flows generated by ultrasound between droplets in water phase facilitate the first reaction by attacking ethylenediamine (water phase) to carbon–sulfur double bond of CS$_2$ (oil phase). Under sonication, the product of first reaction can polymerize and produces H$_2$S (reaction 2). It reacts very fast with cadmium ion present in the solution and leads to CdS. This fact, ultrasound affects the nucleation process of the nano-particles. The total number of nano-particles is correlated with the number of nuclei formed which also corresponds to the rate of hydrogen sulfide formation [40]. In other words, the implosion of the bubble causes many local hot spots in the solution and promotes the reactions.

As a result, the formation, growth and crystallization of CdS nuclei are accelerated under these conditions. In addition, the polymer molecule produced in the second reaction may bridge the oil droplets and water at the CS$_2$–water surface to prevent the agglomeration of the droplets (this mechanism has completely stated in our recent work [28]).

Then by adding TTIP, the rate of hydrolysis of TTIP became highly accelerated in several orders in the presence of ultrasound [25]. Rapid synthesis with uniform deposition of TiO$_2$ on CdS nanoparticles under the described sonochemical conditions might be attributed to the physical and chemical effects of cavitation. The removal of surface contaminants by cavitation causes uniform clusters [18]. On the other hand, the shock waves and turbulent flows as the consequence of microbubble collapses can drive nanoparticles together at velocities of hundreds of meters per second [32] which lead to the formation of core–shell nanoparticles (Fig. 8).

4. Conclusion

In summary, CdS–TiO$_2$ core–shell nano-composites are successfully synthesized at low-temperature through a combination of ultrasound and microemulsion without surfactant. The crystalline phases of TiO$_2$ and CdS in the resulting particles were anatase and hexagonal, respectively. The depth of coated TiO$_2$ onto CdS nanoparticles can be controlled in nano-scale by this method. The average depth was about 1.1 nm under the described conditions. In addition, the optical investigations revealed a red-shift of absorption by increasing the amount of TiO$_2$ in the composite nanoparticles. This observation provides a good indication of tuning the visible absorption of CdS/TiO$_2$ core–shell nanocomposites. The size of nanoparticles can also be controlled by changing the reactant concentrations. Furthermore, the key point of this work is to achieve the core–shell nanoparticles in the presence of ultrasound without additives. Easier workup, shorter reaction time, better crystallinity, better control and higher speed of core–shell formation with uniform shape can be considered as advantageous of this work. This is due to the cavitation process which drives nanoparticles together at high velocities and lead to the formation of core–shell nanoparticles. In addition, the intense local heating can enhance the crystallinity of the nano-particles.

References

[1] J.S. Jang, S.M. Ji, S.W. Bae, H.C. Son, J.S. Lee, Optimization of CdS/TiO$_2$ nano-bulk composite photocatalysts for hydrogen production from Na$_2$S/Na$_2$SO$_3$ aqueous electrolyte solution under visible light ($\lambda \geqslant$ 420 nm), J. Photochem. Photobiol. A: Chem. 188 (2007) 112–119.
[2] M. Shalom, S. Dor, S. Rúhle, L. Grinis, A. Zaban, Core/CdS quantum dot/shell mesoporous solar cells with improved stability and efficiency using an amorphous TiO$_2$ coating, J. Phys. Chem. C 113 (2009) 3895–3898.
[3] S. Anandan, F. Grieser, M. Ashokkumar, Sonochemical synthesis of Au–Ag core–shell bimetallic nanoparticles, J. Phys. Chem. C 112 (2008) 15102–15105.
[4] Y. Liu, F. Xin, F. Wang, S. Luo, X. Yin, Synthesis, characterization, and activities of visible light-driven Bi$_2$O$_3$–TiO$_2$ composite photocatalysts, J. Alloy. Compd. 498 (2010) 179–184.
[5] C. Wang, H. Zhang, J. Zhang, M. Li, H. Sun, B. Yang, Application of ultrasonic irradiation in aqueous synthesis of highly fluoresent CdTe/CdS core-shell nanocrystals, J. Phys. Chem. C 111 (2007) 2465–2469.
[6] R. Brahimi, Y. Bessekhouad, A. Bouguelia, M. Trari, Visible light induced hydrogen evolution over the heterosystem Bi$_2$S$_3$/TiO$_2$, Catal. Today 122 (2007) 62–65.
[7] Y. Bessekhouad, D. Robert, J.V. Weber, Bi$_2$S$_3$/TiO$_2$ and CdS/TiO$_2$ heterojunctions as an available configuration for photocatalytic degradation of organic pollutant, J. Photochem. Photobiol. A: Chem. 163 (2004) 569–580.
[8] S.-C. Lo, C.-F. Lin, C.-H. Wub, P.-H. Hsieh, Capability of coupled CdSe/TiO$_2$ for photocatalytic degradation of 4-chlorophenol, J. Hazard. Mater. B114 (2004) 183–190.
[9] R. Brahimi, Y. Bessekhouad, A. Bouguelia, M. Trari, Improvement of eosin visible light degradation using PbS-sensitized TiO$_2$, J. Photochem. Photobiol. A: Chem. 194 (2008) 173–180.
[10] N.R. Jana, X.G. Peng, Single-phase and gram-scale routes toward nearly monodisperse Au and other noble metal nanocrystals, J. Am. Chem. Soc. 125 (2003) 14280–14281.

[11] W.Z. Wang, I. Germanenko, M.S. El-Shall, Room-temperature synthesis and characterization of nanocrystalline CdS, ZnS, and $Cd_xZn_{1-x}S$, Chem. Mater. 14 (2002) 3028–3033.

[12] J.P. Cheng, R. Ma, D. Shi, F. Liu, X.B. Zhang, Rapid growth of magnetite nanoplates by ultrasonic irradiation at low temperature, Ultrason. Sonochem. 18 (2011) 1038–1042.

[13] L.M. Cubillana-Aguilera, M. Franco-Romano, M.L.A. Gil, I. Naranjo-Rodríguez, J.L. Hidalgo-Hidalgo de Cisneros, J.M. Palacios-Santander, New, fast and green procedure for the synthesis of gold nanoparticles based on sonocatalysis, Ultrason. Sonochem. 18 (2011) 789–794.

[14] N.A. Dhas, K.S. Suslick, Sonochemical preparation of hollow nanospheres and hollo nanocrystals, J. Am. Chem. Soc. 127 (2005) 2368–2369.

[15] D.J. Flannigan, K.S. Suslick, Plasma formation and temperature measurement during single-bubble cavitation, Nature 434 (2005) 52–55.

[16] K.S. Suslick, G.J. Price, Applications of ultrasound to materials chemistry, Annu. Rev. Mater. Sci. 29 (1999) 295–326.

[17] M.M. Mdeleni, T. Hyeon, K.S. Suslick, Sonochemical synthesis of nanostructured molybdenum sulfide, J. Am. Chem. Soc. 120 (1998) 6189–6190.

[18] K. S. Suslick, S. J. Doktycz, In advances in sonochemistry; Mason, T. J., Ed.; JAI Press: New York, 1 (1990) 197–230.

[19] W. Huang, X. Tang, Y. Wang, Y. Koltypin, A. Gedanken, Selective synthesis of anatase and rutile via ultrasound irradiation, Chem. Commun. (2000) 1415–1416.

[20] V.G. Pol, M. Motiei, A. Gedanken, J. Calderon-Moreno, Y. Mastai, Sonochemical deposition of air-stable iron nanoparticles on monodispersed carbon spherules, Chem. Mater. 15 (2003) 1378–1384.

[21] N. Ghows, M.H. Entezari, Fast and easy synthesis of core-shell nanocrystal (CdS/TiO_2) at low temperature by micro-emulsion under ultrasound, Ultrason. Sonochem. 18 (2011) 629–634.

[22] A.L. Morel, S.I. Nikitenko, K. Gionnet, A. Wattiaux, J. Lai-Kee-Him, C. Labrugere, B. Chevalier, G. Deleris, C. Petibois, A. Brisson, M. Simonoff, Sonochemical approach to the synthesis of $Fe3O4@SiO2$ core−shell nanoparticles with tunable properties, acs nano 2 (2008) 847–856.

[23] J.P. Park, S.K. Kim, J.Y. Park, S. Ahn, K.M. Ok, H.-Y. Kwak, I.-W. Shim, Coating of TiO_2 nanoparticles with PbS thin films and preparation of PbS nanoparticles using a one-pot sonochemical reaction under the multibubble sonoluminescence conditions, Thin Solid Films 517 (2009) 6663–6665.

[24] P. Wang, L. Wang, B. Ma, B. Li, Y.J. Qiu, TiO_2 surface modification and characterization with nanosized PbS in dye-sensitized solar cells, J. Phys. Chem. B 110 (2006) 14406–14409.

[25] S.S. Lee, K.W. Seo, S.H. Yoon, I.-W. Shim, K.-T. Byun, H.-Y. Kwak, CdS Coating on TiO_2 nanoparticles under multibubble sonoluminescence Condition, Bull. Korean Chem. Soc. 26 (2005) 1579–1581.

[26] M.H. Entezari, N. Ghows, Micro-emulsion under ultrasound facilitates the fast synthesis of quantum dots of CdS at low temperature, Ultrason. Sonochem. 18 (2011) 127–134.

[27] N. Ghows, M.H. Entezari, Ultrasound with low intensity assisted the synthesis of nanocrystalline TiO_2 without calcinations, Ultrason. Sonochem. 17 (2010) 878–883.

[28] N. Ghows, M.H. Entezari, A novel method for the synthesis of CdS nanoparticles without surfactant, Ultrason. Sonochem. 18 (2011) 269–275.

[29] C. Han, Z. Li, J. Shen, Photocatalytic degradation of dodecyl-benzenesulfonate over TiO_2–Cu_2O under visible irradiation, J. Hazard. Mater. 168 (2009) 215–219.

[30] Raghvendra S. Yadav, Priya Mishra, Rupali Mishra, Manvendra Kumar, Avinash C. Pandey, Growth mechanism and optical property of CdS nanoparticles synthesized using amino-acid histidine as chelating agent under sonochemical process Ultrasonics Sonochemistry 17(2010) 116–122.

[31] D.L. Liao, B.Q. Liao, Shape, size and photocatalytic activity control of TiO_2 nanoparticles with surfactants, J. Photochem. Photobiol. A: Chem. 187 (2007) 363–369.

[32] D. Radziuk, D. Grigoriev, W. Zhang, D. Su, H. Móhwald, D. Shchukin, Ultrasound-assisted fusion of preformed gold nanoparticles, J. Phys. Chem. C 114 (2010) 1835–1843.

[33] M. Ashokkumar, M. Hodnett, B. Zeqiri, F. Grieser, G.J. Price, Acoustic emission spectra from 515 kHz cavitation in aqueous solutions containing surface-active solutes, J. Am. Chem. Soc. 129 (2007) 2250–2258.

[34] S. Ito, S. Inoue, H. Kawada, M. Hara, M. Iwasaki, H. Tada, Low-temperature synthesis of nanometer-sized crystalline TiO_2 particles and their photoinduced decomposition of formic acid, J. Coll. Interface Sci. 216 (1999) 59–64.

[35] M. Ashokkumar, L.A. Crum, C.A. Frensley, F. Grieser, T.J. Matula, W.B. McNamara III, K.S. Suslick, Effect of solutes on single-bubble sonoluminescence in water, J. Phys. Chem. A 104 (2000) 8462–8465.

[36] K.S. Suslick, S.B. Choe, A.A. Cichowlas, M.W. Grinstaff, Sonochemical synthesis of amorphous. Iron, Nature 253 (1991) 414–416.

[37] S. Avivi (Levi), O. Palchik, V. Palchik, M.A. Slifkin, A.M. Weiss, A. Gedanken, Sonochemical synthesis of nanophase indium sulfide, Chem. Mater. 13 (2001) 2195–2200.

[38] H. Wang, J.R. Zhang, J.J. Zhu, Sonochemical preparation of lead sulfide nanocrystals in an oil-in-water microemulsion, J. Cryst. Growth 246 (2002) 161.

[39] X. Fu, D. Wang, J. Wang, H. Shi, C. Song, High aspect ratio CdS nanowires synthesized in microemulsion system, Mater. Res. Bull. 39 (2004) 1869–1874.

[40] K. Okitsu, A. Yue, S. Tanabe, H. Matsumoto, Y. Yobiko, Formation of colloidal gold nanoparticles in an ultrasonic field: control of rate of gold(III) reduction and size of formed gold particles, Langmuir 17 (2001) 7717–7720.